

Integrating geospatial data and analytic hierarchy process for flood-prone zones mapping in the Upper Draa basin, Morocco

Lahcen Goumghar^{1*}, Rahma Fri¹, Soufiane Hajaj², Soufiane Taia³,
Bouabid El Mansouri¹

¹ Natural Resources and Sustainable Development Laboratory, Faculty of Sciences, Ibn Tofail University, Kenitra 133, Morocco

² Laboratory of Geomatic, Georesources and Environment, Faculty of Sciences and Techniques, Sultan Moulay Slimane University, 23000 Beni Mellal, Morocco

³ National Thematic Institute for Research in Water, Ibn Zohr University, Morocco

* Corresponding author's e-mail: lahcen.goumghar@gmail.com

ABSTRACT

In this study, we conducted a comprehensive assessment of flood susceptibility in the northern part of the large-scale Draa Oued Noun Basin DON using the modeling approach analytic hierarchy process (AHP). These techniques were applied to integrate key hydrogeological, geomorphological, and geological parameters, identifying areas that are heightened in flood-prone. The study evaluates the accuracy and reliability of the method in addressing several environmental parameters uncertainty and variability while exploring their combined potential to enhance flood assessment. The results indicate that flood-prone areas are categorized as follows: very low (22.78%), low (26.25%), medium (23.92%), high (16.45%), and very high (10.59%) susceptibility zones. The performance evaluation of AHP-based modeling confirmed its strong discriminatory power, with an AUC value of 0.882 that could identify flood-prone zones with high precision. The current study findings provide actionable recommendations to inform flood mitigation strategies and land-use planning. This study strengthens the long-term management of water supplies and improves disaster resilience, tackling the escalating impacts of environmental shifts and rising anthropogenic pressures.

Keywords: flood prone mapping, Semi-Arid Basin, Draa-Ouadnoun, Morocco, AHP-MCDM model-based assessment.

INTRODUCTION

Flooding is one of the most common, perilous, and devastating natural disasters, consistently threatening various places globally, and it represents one of the most urgent environmental hazards, presenting substantial risks to people, infrastructure, and crops and ecosystems (Tanguy, 2012). Flooding has become a growing threat due to expanding settlements in vulnerable areas and intensified extreme weather events driven by climate change. Increased localized storms now trigger rapid and severe flash floods, posing significant risk (Echogdali et al., 2018). In the Draa-Ouadnoun Basin, Southern Morocco, extreme rainfall variability, combined with complex topographical and geomorphological features

(Khaddari et al., 2022; Khettouch et al., 2023), has led to increasing vulnerability to flood events. These challenges necessitate advanced approaches to delineate flood-prone zones, enabling effective flood management and mitigation strategies. The delineation of flood-prone regions requires the integration of multiple geological, hydrological, and geomorphological factors in this complex environment.

Recent advancements in flood assessment methods have mostly focused on the incorporation of machine learning (ML) methods, bivariate statistical analysis, and multi-criteria decision-making (MCDM) frameworks. Among these approaches, artificial neural networks (ANNs) (Aghenda et al., 2024; Khoirunisa et al., 2021), support vector machines (SVM) (Shafapour

Tehrany et al., 2019; Shikhteymour et al., 2023) and, decision trees (DTs) (Mashaly & Ghoneim, 2018). Bivariate statistical analysis was one of the most used approaches for studying flood susceptibility assessments, with the ability to establish relationships between the incidence of floods and the factors that influence them (Pusdekar & Dudul, 2024), using models such as the frequency ratio (FR) (Akay & Baduna Koçyiğit, 2024; Saha et al., 2022; S. Samanta et al., 2018), certainty factor (CF) (Cao et al., 2020), index of entropy (IoE) (Ivan Ulloa et al., 2020), weights of evidence (Sarker et al., 2024), and statistical index (SI) method (Muthu & Ramamoorthy, 2024). However, because statistical methods rely on variables derived from linear assumptions, they frequently fail to adequately handle the complex, non-linear dynamics of floods, potentially oversimplifying the complicated interactions among influencing components (Costache & Bui, 2020; Tehrany, Pradhan, & Jebur, 2015; Tehrany, Pradhan, Mansor, et al., 2015). MCDM models have garnered substantial attention in flood-related studies due to their robust capability to incorporate and analyze multiple criteria, enabling comprehensive and balanced evaluations of flood susceptibility and risk (Song & Chung, 2016). They can be used for several aims including flood susceptibility mapping (FSM) (Roy et al., 2021), flood hazard zonation (Akay & Baduna Koçyiğit, 2024; Das, 2018), Mapping flood vulnerability (Dey et al., 2024), flood risk mapping (Radwan et al., 2019), flash flood analysis (Costache & Bui, 2020), forecasting floods (Teh Noranis et al., 2019), and Among MCDM techniques, the most widely used are the analytical hierarchy process (AHP) (Das & Gupta, 2021; Mitra et al., 2022; Wang et al., 2018). AHP (Saaty, 1980), a MCDM approach, is among the most widely utilized techniques in flood susceptibility mapping (Leta & Adugna, 2023), since it enables a systematic comparison of disparate criteria based on their relative importance. AHP assigns weights to different flood susceptibility factors, including rainfall intensity, slope, and land use, incorporating expert knowledge in highlighting those very crucial factors for flood risk (Samanta et al., 2018; Zou et al., 2013). This method adds a great value to the Draa-Ouadnoun Basin, where expertise judgment will be crucial in determining how the elements are ranked. influencing flooding according to the hydro-meteorological conditions of the area under consideration.

The hydrological setting of the Draa-Ouadnoun Basin is so complicated due to topographical and lithological variations as well as great spatial variability in rainfall and distribution heterogeneity. This study addresses the critical gap in flood susceptibility mapping within the Upper Draa Basin (UDB), a region that have recently experienced a severe flash floods, via integrating RS data and AHP-MCDM with GIS. It provides a structured, expert-driven methodology to assess flood susceptible region in an efficient as well as sustainable manner, accounting for the basin's complex topography, lithology, and rainfall variability. The research contributes in advancing flood management by offering a transferable framework tailored to data-scarce, and semi-arid environments, enabling more effective decision-making strategies. It therefore becomes very important to establish which approach best describes this complication in order to have a realistic susceptibility flood map. Taking precedence to render help toward decision-makers coming up with strong policies in the management of floods, resource allocation planning, and sustainability measures concerning desert and semi-arid regions that are vulnerable to flooding. The methodology takes looks at how MCDM techniques can be made applicable to deal with the hydrological variability in that respect. The results are intended to feed into flood susceptibility mitigation and planning processes in similar hydrologically problematic regions. Accordingly, employing AHP, which can include expert-driven prioritization. Performance evaluation under the current data conditions in such environment will help to identify and assess flood susceptibility mapping. The primary goals of this research are:

- To assess and map areas that are at high risk of flooding via analytic hierarchy process within the Upper Draa Basin, regarding their spatial precision and efficiency.
- To discuss how these MCDM-based modeling may provide information on the elaboration of a sustainable regional approach to flood management, especially for the most prone flood area.

The attainment of these objectives will ensure that a reliable methodology is provided for delineating flood-prone zones while at the same time guaranteeing sound strategies for disaster risk reduction. This research forms part of sustainable flood management planning for both the Draa-Ouadnoun Basin and other similar regions characterized by arid or semi-arid environments.

MATERIALS AND METHODS

Study area

The Draa Oued Noun (DON) watershed, situated between latitudes 32° N and 29.3° N and longitudes 9.88° W and 5.5° W in southern Morocco. it is one of the biggest watersheds of the Kingdom, has an area of greater than 103460 km², covering 1/7 of the total area of Morocco. The DON is bounded by the High Atlas Mountains to the north, the Atlantic Ocean to the west, the Sahara to the south, and Algeria to the east (Fig. 1). In the DON settled agriculture developed around underground water sources and dry riverbeds that flood during the rainy season temperatures are mild and regular, exhibit a semi-arid to arid climate, with an annual average of 22 °C. The plains receive 100 mm of rainfall annually, whereas the High Atlas Mountains receive 600 mm. There are four main sub-watersheds located in the DON which are the Upper Drâa which is the current study area (Fig. 1), Middle Drâa, Lower Drâa, and Guelmim.

Methods

A bibliographic analysis of more than 400 scientific articles published between 2000 and 2025 was conducted to identify the key mechanisms and factors associated with floods,

specifically in the context of applying the AHP method. This approach allowed the identification of several closely related and frequently studied themes within the literature on flood management. The findings, illustrated in Figure 2, highlight the main key factors within flood investigation such as vulnerability, risk and susceptibility, represented as circles of varying sizes. The size of each circle reflects the relative significance of a concept within the broader theme, while their proximity to the center indicates their connection to the central topic, namely “flood management using AHP” (Fig. 2).

Furthermore, the current study methodology for determining flood susceptibility in the Upper Draa watershed is illustrated in Figure 3. The method combines spatial remote sensing, GIS, and MCDM. Overall, the flowchart in Figure 2 provides a concise synopsis of the methodology employed in this investigation, highlighting the integration of multiple data typologies. This study initiates data acquisition and preparation. Seven key factors influencing flood susceptibility were incorporated into the analysis: precipitation, lithology, land use, elevation, slope, flow accumulation, and distance to the river. These elements were chosen in light of an extensive assessment of the literature and their relevance to similar studies conducted in southern Moroccan territory (Khaddari et al., 2023).

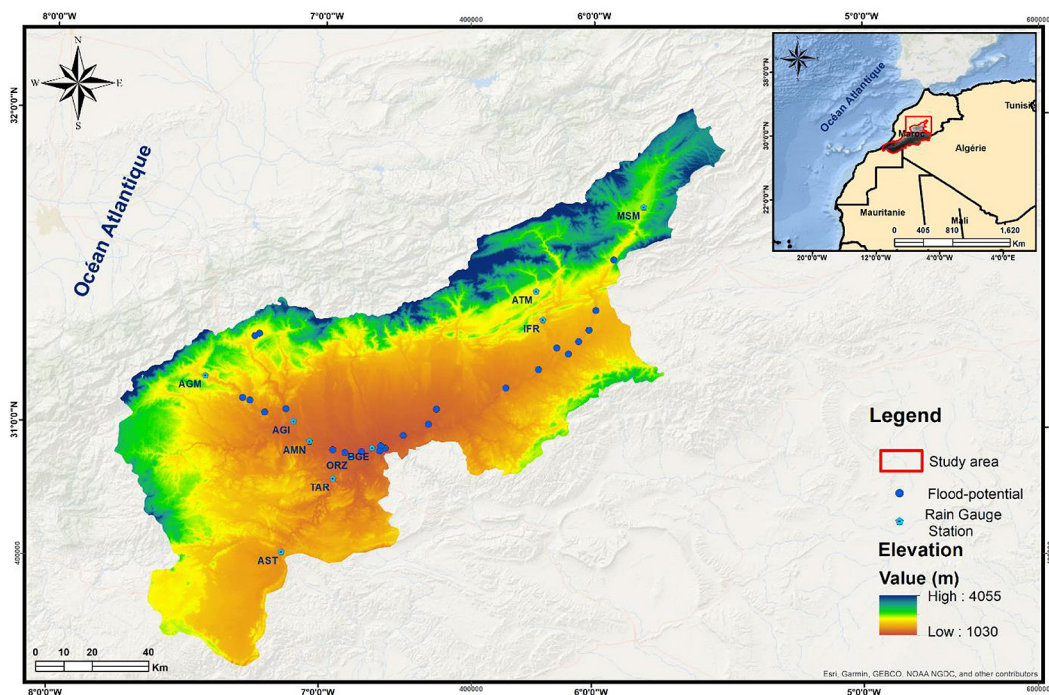


Figure 1. Geographical situation of the study area Upper Draa basin and in-situ gauge stations.

aggregated using a mathematical formulation integrated into the GIS, leading to the generation of a final flood susceptibility map (FSM). This map was validated using the receiver operating characteristic (ROC) curve, a widely adopted statistical method for assessing the performance of predictive models. Field control points were utilized to compute the area under the curve (AUC), ensuring the reliability and accuracy of the produced map.

Data acquisition and preparation

The methods used offer several advantages, including, the production of accurate flood prone estimates without relying solely on empirical models or limited historical data. These methods effectively combine the area’s specific flood susceptibility with the critical factors required for optimal management of flood-prone. Furthermore, this knowledge-driven approach significantly reduces time and costs compared to conventional methods. The necessary data for the current study were extracted from a variety of sources (Table 1). A field campaign was carried out to evaluate flood risks within the study area. This mission allowed for the identification and documentation of areas affected by flooding while analyzing the factors that exacerbate their occurrence.

MCDM-modeling method

The analytic hierarchy process is a structured and systematic multi-criteria decision-making approach that facilitates the evaluation and prioritization of alternatives based on multiple weighted criteria. Developed by Saaty, AHP relies on a

hierarchical decomposition of the decision problem and pairwise comparisons of its constituent elements. This method is widely applied across various scientific domains in its original or in various modified versions, including risk management, land-use planning, environmental studies, and strategic decision-making, due to its capability to integrate both qualitative and quantitative criteria (Das, 2018; El Jazouli et al., 2019; Khosravi et al., 2021; Nithya et al., 2019; Panchal & Shrivastava, 2022; Radwan et al., 2019; Saremi et al., 2024; Swain et al., 2020). Its robustness makes it particularly valuable in complex decision-making scenarios where multiple factors and competing priorities must be considered.

AHP

The goal of the current investigation on flood prone mapping (FPM) cannot be effectively attained by relying on only one parameter or evaluation metric, as the physical environment is inherently multi-faceted. Therefore, it is essential to consider multiple perspectives to inform decision-making (Saaty, 1990). In this context, the AHP is mainly utilized as a semi-qualitative method for supporting strategic planning. AHP involves performing pairwise comparisons of the causal factors to assign weights based on their relative importance (Saaty, 1990). The latter was extensively used in flood assessment and FPM, owing to its flexibility and robustness. It permits adjusting factors weighting, enhancing the robustness of the decision support framework (Saaty, 1990; d’Avignon & Sauvageau, 1996; El Morjani, 2002; Jari et al., 2022; Wang et al., 2018). The current research employs the

Table 1. Datasets utilized for the mapping of flood prone within the Upper Drâa watershed.

Data type	Resolution	Year	Reference
ASTER-DEM	30 meters	2009	https://earthexplorer.usgs.gov
Slope	30 meters	2009	Generated from DTM (ASTER-DEM).
Flow accumulation	30 meters	2009	Generated from DTM (ASTER-DEM).
Hydrographical network	30 meters	2009	Generated from DTM (ASTER-DEM).
Sentinel-2 satellite Simage	VNIR 10 meters	2024	https://earthexplorer.usgs.gov .
LU/LC	30 meters	2024	Obtained from Sentinel-2 processing.
Lithological data	30 meters	1951	Extracted from the geological map of Upper Drâa at a scale of 1:200,000.
Precipitation	30 meters	2000–2024	A network of meteorological stations.
Flood sites	Shapefile	2006–2024	Draa-Oued Noun Hydraulic Watershed Agency (DONHBA) A six-day field mission was conducted to study flood risks in the study area from 25 to 31 October .2024

AHP approach and follows a structured process, consisting of three key stages:

1. Standardizing as well as weighting criteria, where the various criteria are normalized and assigned relative weights on the basis of their importance to flood occurrence;
2. Consistency check, to warrant the fact that the established pairwise comparisons maintain logical consistency, as per Saaty’s consistency ratio;
3. Aggregation of criteria, where the weighted criteria are combined to form an overall flood risk assessment, providing a comprehensive and balanced evaluation of the zone’s flooding susceptibility. This approach enables a more nuanced with reliable decision-making process, factoring in the complexity of flood risk assessment.

Standardization/weighting of evaluation criteria

After identifying and hierarchically ranking the flood susceptibility factors (including flow accumulation, lithology, proximity to hydrographical network, altitude, slope, LULC, and precipitation) (Morjani, 2011; Khaddari et al., 2023, El Morjani, 2002; Hammami et al., 2019; Yurdakul,

2004), a pairwise comparison matrix (PCM) is established using every component to evaluate the relative importance of each parameter. These evaluations are quantified on a numerical scale ranging from 1 to 9, where 1 signifies the lowest level of significance and 9 characterises the highest degree of importance (Table 2).

The used approach involves developing a hierarchical pairwise comparison with a seven*seven matrix, with diagonal values fixed at 1 (Table 3). Each row is compared against the corresponding column to determine relative importance and determine evaluation scores. For instance, if flow accumulation (FC) is deemed significantly more important than LULC, it would receive a score of 5.

Inverse relationship is represented in the corresponding cell (e.g., 1/3 for land use/land cover (LULC) in relation with FC (Khaddari et al., 2023).

Next, a normalized index It is determined by dividing the total score by the score of the individual factor (refer to Table 3). Based on these individual weights, a total weight (W) of 1 is distributed across the seven parameters (Table 4) (Cao et al., 2020). The Table 4 presents the

Table 2. Articulation and quantification of the comparative significance of a dual set of criteria.

A verbal representation of the relative importance of one criterion in comparison to another	Numerical
Even more (even more important)	1
Moderately more	3
Strongly more	5
Very much more	7
Extremely more	9
Moderately less	1/2
Strongly less	1/5
Very less	1/7
Extremely less	1/9

Table 3. Matrix of pairwise comparisons for flood causative factors.

Parameter	FC	PR	DD	ELE	SLOPE	LULC	LITH
FC	1.00	5.00000	5.00000	5.00000	5.00000	7.00000	7.00000
PR	1/5	1.00	3.00000	3.00000	3.00000	5.00000	6.00000
DD	1/5	1/3	1.00	3.00000	5.00000	5.00000	6.00000
ELE	1/5	1/3	1/3	1.00	3.00000	3.00000	4.00000
SLOPE	1/5	1/3	1/5	1/3	1.00	3.00000	3.00000
LULC	1/3	1/5	1/5	1/3	1/3	1.00	3.00000
LITH	1/5	1/6	1/6	1/4	1/3	1/3	1.00

Note: FC – flow accumulation, DD – distance from the hydrographic network, ELE – elevation, LITH – lithology, PR – precipitation.

Table 4. Standardized flood parameters through the hierarchical analysis process

Parameter	FC	PR	DD	ELE	SLOPE	LULC	LITH	Wi
FC	0.43	0.68	0.51	0.39	0.28	0.29	0.23	40.0%
PR	0.09	0.14	0.30	0.23	0.17	0.21	0.20	19.0%
DD	0.09	0.05	0.10	0.23	0.28	0.21	0.20	16.5%
ELE	0.09	0.05	0.03	0.08	0.17	0.12	0.13	9.5%
SLOPE	0.09	0.05	0.02	0.03	0.06	0.12	0.10	6.5%
LULC	0.14	0.03	0.02	0.03	0.02	0.04	0.10	5.4%
LITH	0.09	0.02	0.02	0.02	0.02	0.01	0.03	3.0%
Lambda max	7.489							
CI	0.073							
CR	0.06							

Note: Wi – weight.

outcomes of a hierarchical analysis process employed to standardize flood parameters, and their derived weights. The values in the table represent the relative importance of each parameter compared to others, with FC as the most influential factor with a weight of 40.0%, followed by RF (19.0%) and DD (16.5%). Other parameters, ELE, Slope, LULC, and LITH, relatively exhibit progressively lower weights.

The Table 5 outlines the classification of each causal factor, the intensity ratings, and the weights derived using the AHP. Each causal factor is categorized into distinct classes based on its contribution to flood occurrence, with corresponding intensity ratings (from 1 for “very low” to 5 for “very high”) and weights that reflect their relative importance in the overall flood occurrence assessment.

Table 6 presents the values of the random index (RI), which are determined by the number of factors involved (Saaty & Vargas, 2012). Within this investigation, seven factors have been considered, with the RI = 1.32.

In order to calculate consistency index, Equation 1 has been implemented:

$$I = \frac{\lambda_{max} - n}{n - 1} \tag{1}$$

where: λ_{max} is the maximum eigenvalue, and n denotes the number of criteria. In this study, the consistency index (CI) has been computed using $n=7$, and $\lambda_{max} = 7.35$.

Randomized index used as displayed in Table 6 is 1.32. Consequently, the calculated consistency ratio (CR) is 0.04, which is significantly below the threshold of 0.1. This result confirms that the

pairwise comparison matrix (PCM) demonstrates an acceptable level of consistency.

After defining the evaluation criteria factors and assigning weighting coefficients (Table 5), the next step is to combine these layers using a mathematic operation for the Initial grouping of criteria into a unique layer (Eq. 2). The integration of weighted factors in raster format is performed through the raster calculator tool integrated within ArcGIS 10.5.

$$A = \sum_{i=1}^n P_i V_i \tag{2}$$

where: A represents the aggregation of criteria, n is the number of criteria, P_i denotes the weight of criterion i, and V_i is the standardized value of factor i; the application of this formula is shown in Equation 3.

$$A = (W_{i_{FlowAcc}} \times FlowAcc) + (W_{i_{Lith}} \times Lithology) + (W_{i_{Slop}} \times Slope) + (W_{i_{DD}} \times D_{RH}) + (W_{i_{LULC}} \times Land\ use\ Land\ cover) + (W_{i_{Pre}} \times Precip_{mean}) + (W_{i_{ELE}} \times Elevation) \tag{3}$$

Consistency check

Consistency check (CR) is a mathematical indicator used to evaluate the reliability of decisions in a pairwise comparison process (Saaty, 1977). A CR value below 0.1 indicates acceptable consistency, while values exceeding this threshold suggest inconsistencies within the comparison matrix. In this study, the CR of the analytic hierarchy process (AHP) matrix was determined using the formula provided in Equation 4.

$$CR = \frac{CI}{RI} \tag{4}$$

where: CR is consistency ratio; CI is consistency index; RI is randomized index.

Table 5. Classification and weights of flood prone decision factors determined using the AHP method

Causal factors	Class	Intensity	Rating	Weight
Flow accumulation (pixel)	6.056e+6–1.643e+7	VH	5	0.44
	3.222e+6–6.055e+6	H	4	
	1.676e+6–3.221e+6	M	3	
	5.154e+5–1.675e+6	L	2	
	0.000–5.153e+5	VL	1	
Precipitation (mm)	223.4–258.4	VH	5	0.19
	191.0–223.4	H	4	
	163.4–190.9	M	3	
	136.4–163.3	L	2	
	101.9–139.3	VL	1	
Density hydrographic network (No/km ²)	1.2–2.1	VH	5	0.17
	0.84–1.2	H	4	
	0.51–0.84	M	3	
	0.21–0.51	L	2	
	0–0.21	VL	1	
Elevation	1 000–1 400	VH	5	0,09
	1 400–1 700	H	4	
	1 700–2 200	M	3	
	2 200–2 700	L	2	
	2 700–4 100	VL	1	
Slope	<2.3	VH	5	0.07
	2.3–5.2	H	4	
	5.2–8.7	M	3	
	8.7–13	L	2	
	13–49	VL	1	
LULC	Wt, Bt, Oa	VH	5	0.054
	Veg, Cp	H	4	
	BL	M	3	
	Clt	L	2	
	SP	VL	1	
Lithology	Quartzite and sandstone	VH	5	0,03
	Dolomite, limestone, sandstone with clay intercalation, shale, and siltstone.	H	4	
	fractured limestones, Tuffs, shales, and alluvial cone.	M	3	
	Terrace, scree, lacustrine limestone, and old alluvial cone.	L	2	
	Recent Reg and Alluvium	VL	1	

Note: VH – very high, H – high, M – medium, L – low, VL – very low.

Table 6. The used RI values in the RC calculation.

Number of criteria (n)	1	2	3	4	5	6	7	8	9	10
Randomized index (RI)	0	0	0.58	0.90	1.12	1.24	1.32	1.41	1.45	1.49

The consistency of the AHP model for flood-prone mapping was checked using a consistency check. The calculated maximum eigenvalue λ_{max} was 7.489 and the CI was found to be 0.073. With a CR of 0.06, below the threshold

of 0.1, the results confirm the satisfactory consistency of the pairwise comparison matrix. This will ensure that the weighting scheme applied to factors influencing flood susceptibility is reliable and robust.

RESULTS

Spatial variation of the thematic layers

Elevation

Lower altitudes, particularly flat areas, tend to experience a higher susceptibility of flooding due to reduced drainage capacity (Vignesh et al., 2021). We employed a DEM derived from ASTER data accessible at <https://earthexplorer.usgs.gov>. This DEM boasts a spatial resolution of 30 meters. To encompass the entire Upper Drâa watershed, we downloaded, processed, rectified six scenes, and georeferenced them using Lambert's Conformal Conical Projection for southern Morocco. Subsequently, the watershed boundaries were automatically delineated and visually validated against 1:100,000 scale topographic map. The Upper Drâa watershed exhibits significant topographic variation, with elevations ranging from 1000 meters to a peak of 4100 meters in the northwestern area of the watershed (Figure 4a).

LULC

Human activities, including urban development and agricultural expansion, and play a critical role in influencing flood occurrence. These activities frequently result in the proliferation of impervious surfaces, which impede natural water infiltration and exacerbate surface runoff (El Morjani et al., 2016). As a result, a clear relationship exists between land-use practices and The distribution of the areas susceptible to flooding, as documented in previous studies (Apollonio et al., 2016; Barkey et al., 2020). In this study, the LULC map is generated using Sentinel-2 satellite

imagery, which provides a higher spatial sampling distance of 10 meters in comparison to medium-resolution satellite-derived images. (Çavur et al., 2019). Different land cover categories are clearly delineated, including bare land, buildings, crops, greenhouse crops, water bodies, oases, solar panel areas, and vegetation. Each category is represented using a distinct color, as detailed in the legend. The map effectively highlights the spatial distribution of these classes, with vegetation and bare land appearing to dominate the landscape. Crops and greenhouse areas are concentrated in specific zones, while water bodies and solar panel regions occupy relatively smaller areas. The presence of buildings and oases indicates the human and natural interaction in the region (Figure 4b). LULC map aids for understanding land use dynamics and evaluating the potential influence of these classes on flood and other environmental processes within the watershed. Its high resolution ensures a detailed representation of the spatial patterns, enhancing the reliability of subsequent analyses. Then, this LULC map was classified as follows: highest values (impermeable areas), the medium values, and the lower values (infiltration areas) (refer to Table 5).

Drainage density

Drainage density, first defined by Horton (1932), represents the total streams length within a drainage watershed divided by the watershed's area. It is a fundamental concept in hydrologic analysis, measuring the drainage length per unit area. A high drainage density shows that the drainage basin is highly dissected and that a hydrologic response from a rainfall event will be

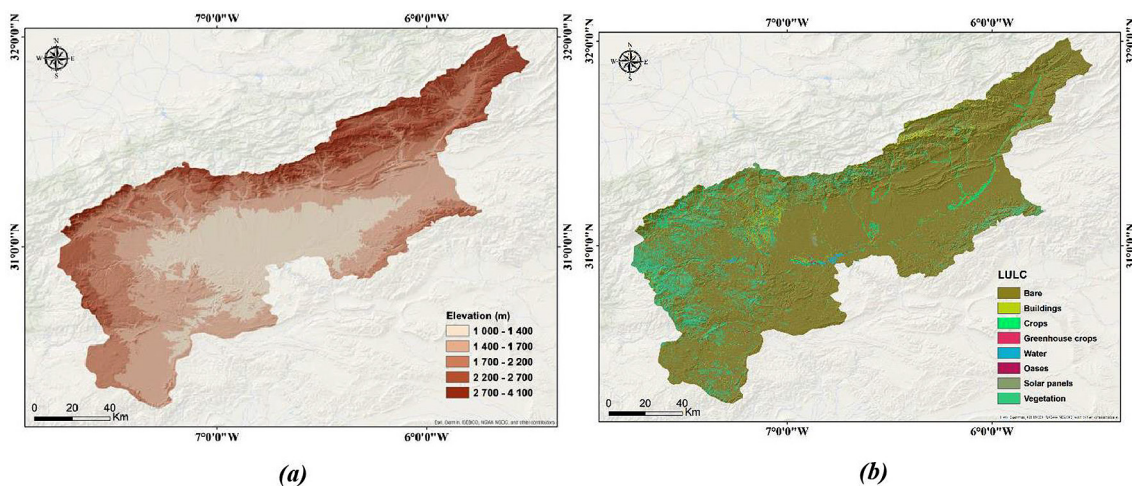


Figure 4. Elevation map (a) and land use and land cover map LULC (b)

fairly quick whereas a low drainage density signifies a weakly drained catchment, which is characterized by a slow hydrologic response (Melton, 1957). The differences in the density of stream networks across the study area influences drainage density values, where, higher values indicate regions with more densely packed streams, potentially influencing factors like runoff rates and erosion potential. Figure 4b displays the drainage density value, which ranges from 0 to 2.1 no/km².

Slope

Slope is a key factor influencing the behaviour of surface water, determining runoff and infiltration. Areas of low gradient tend to enhance the infiltration process, which could lead to a greater danger of flooding due to a decrease in drainage (Ikirri et al., 2022). On the other hand, high slope areas, generally mountainous (upstream), feature a higher runoff rate. Figure 5a Indicates that slope values range from 0 to 49 degrees in the upper stream plains of the Upper Draa watershed, where these values are derived from an elevation raster. This variation in gradient greatly influences the hydrological processes in the watershed (Khaddari et al., 2023).

Flow accumulation

Areas located near flow accumulation paths, especially those with substantial upstream water volumes, have more susceptibility to flood occurrence (Dash & Sar, 2020; Khaddari et al., 2023; Vignesh et al., 2021). The factor of flow accumulation, extracted from the DEM, represents the total flow from all upstream cells channelled into each downslope cell within the resulting image.

High flow accumulation values indicate areas of rigorous flow channels, whereas cells with no flow accumulation correspond to elevated topographical features like ridges or peaks. The resulting flow accumulation thematic layer is then categorised to 5 categories based on the accumulated water volume, with the maximum values corresponding to the lowermost elevations within the studied basin (Figure 6a).

Precipitation

The map illustrates the spatial distribution of average annual rainfall in an upper Draa water sheet. The various colors correspond to different rainfall values, which range from 101.9 to 258.4 mm. Rainfall is clearly gradated on the map, with higher values concentrated in the eastern and western. Near the southern and western borders, the amount of rainfall steadily declines. The regional average yearly rainfall varies significantly, as indicated by the color variations. The regions with the darkest blue hues probably get the most rainfall, whilst those with lighter hues get less.

The Average annual rainfall map was determined through a multi-step process. Firstly, historical rainfall data was collected from meteorological stations within the region. Subsequently, the average annual rainfall for each station was determined by the sum of the whole rainfall recorded annually and dividing it by the year number. Finally, geostatistical techniques, such as Kriging, were employed to interpolate rainfall values between stations, resulting in a continuous surface of average annual rainfall across the entire region (Figure 6b).

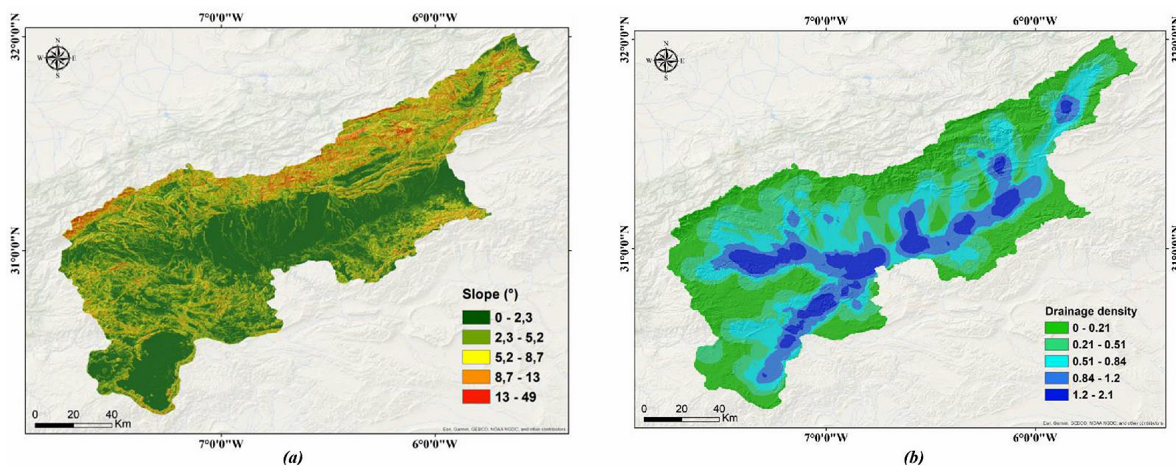


Figure 5. Slope map (a) and drainage density map (b)

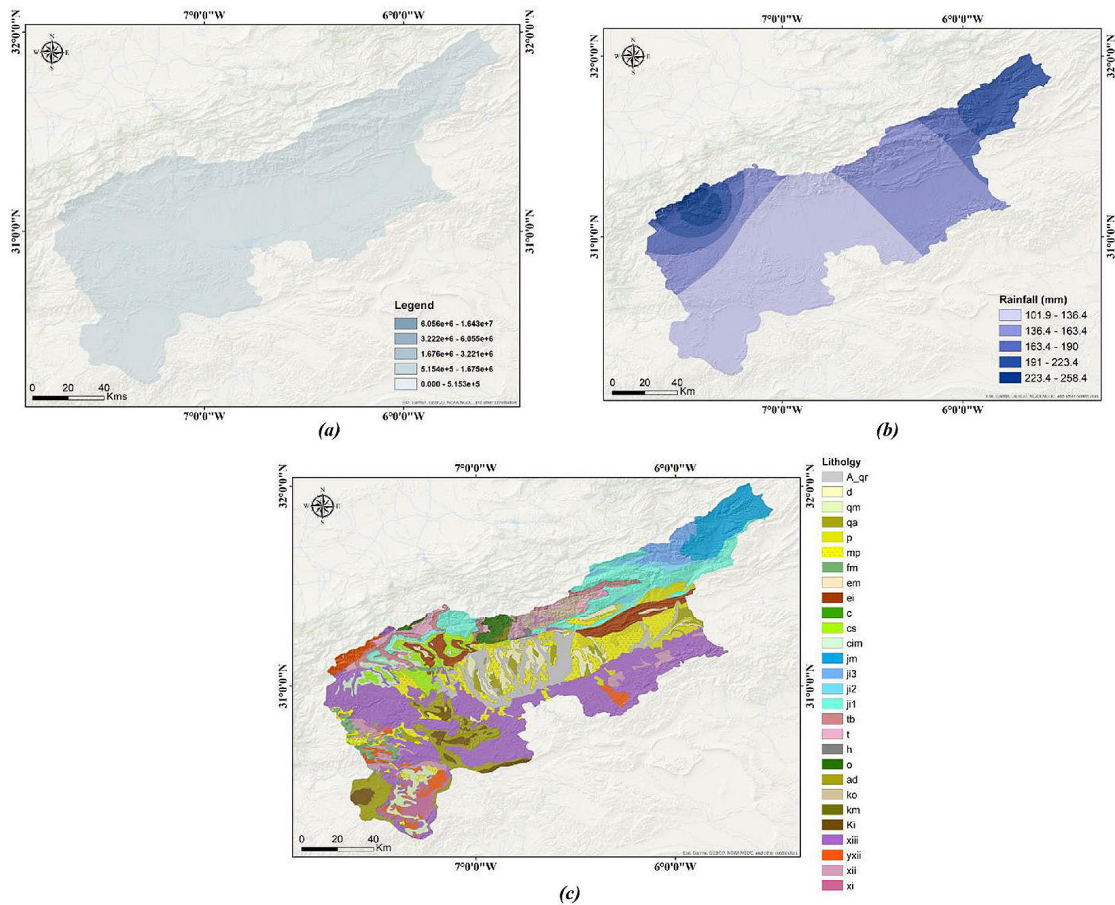


Figure 6. Flow accumulation (a), precipitation (b), and lithology (c). Abbreviations: A-qr: Alluviums, low terraces, D: Sand dunes, qm: Silts, conglomerates, alluviums, qa: Conglomerates (regs, alluvial fans), p: Sandstones, limestones, mp: Sandstones, silicifiedlimestones, fm: Phonolites of Siroua, ems: Marly sandstones, ei: Limestones, sandstones, marly sandstones, c: Limestones, marls, cs: Clayey sands, more or less sandy sandstones, cm: Sandstones, limestones, clays with gypsum, cim: Sandstones, marls, limestones, jm: Marlsand limestones, ji3: Argillaceous-sandy detrital series, ji2: Dolomites and limestones, ji1: Marly-dolomitic series, tb: Doleritic basalts, t: Argillaceous-sandy series, h: Schists, sandy limestones, o: Schists, limestones, ko: Schists, quartzites, km: Schists, sandstones, ki: Limestones, schist-limestones, Ad: Dolomites, wine-colored series, xlll: Volcanic, volcano-detrital series, xll: Volcano-sedimentary series and flysch, xi: Migmatites, micaschists, gneisses

Lithology

The lithological assemblage in the studied region is varied and includes many different types of rock formations. These consist of Quaternary deposits such as conglomerates (qa), sand dunes (D), and alluvium (A-qr). Sandstones, schists (h, o, ko, km), quartzites (ko), dolomites (ji2, Ad), marls (c, cm, jm, ji1), limestones (p, mp, ems, ei, cm, cim, jm), and different volcanic rocks (fm, tb, xlll, xll). Metamorphic rocks such as gneisses, micaschists, and migmatites are also present in the region (Choubert, 1952) (Figure 6c). The region's topography, hydrology, and soil properties are greatly influenced by this varied lithological framework (Devito et al., 2005).

Flood-prone map

After processing all input factors, the AHP-MCDM framework was implemented using the designated formula (Equation 4) to systematically integrate multiple criteria influencing flood susceptibility. The weighted overlay of these factors was performed in a raster environment utilizing the Raster Calculator (Figure 7a), ensuring a spatially explicit representation of flood-prone areas. A thorough visual assessment of the generated outputs revealed that flow accumulation emerged as the most influential determinant of flood risk, given its direct correlation with surface runoff concentration. Additionally, river density and elevation were identified as key contributing factors,

with densely distributed river networks and lower elevation zones exhibiting heightened flood susceptibility. These results are further corroborated by Figure 5 and 6 as well as Figure 1 which presents the spatial distribution of the historic flood-prone zones across the Upper Draa watershed. As shown in Figure 7a, areas classified under the highest flood susceptibility category are predominantly located in the northeastern, the central, and the western sections of the study area, aligning with regions characterized by hydrological constraints and topographical depressions conducive to water retention and rapid runoff accumulation.

The statistical breakdown of flood susceptibility zones, depicted in Figure 7b, provides a quantitative assessment of the spatial extent of each flood susceptibility class. The findings indicate that approximately 75% of the study area falls within the medium, low, or very low flood risk categories, signifying regions with relatively lower vulnerability. Conversely, high and very high-risk zones constitute nearly 26% of the total area, emphasizing the existence of critical flood-prone sections requiring immediate attention. Further validation of these classifications is presented in Figure 7c, which delineates the specific land

coverage for each risk category. Notably, the very high-risk areas span approximately 1,624.17 km², while low-risk zones extend across 4,023.10 km². These insights highlight the necessity of developing robust flood mitigation strategies tailored to the unique hydrological dynamics of the Upper Draa Basin. Effective flood risk management in these highly susceptible areas is imperative to minimize potential damages, support sustainable water resource planning, and enhance regional resilience against extreme hydrological events.

Model performance and validation procedures

The area under the curve metric ranges from 0.5, indicating a random classifier, to 1, representing a perfect classifier, provides a measure of a model’s ability to correctly rank instances based on their predicted class probabilities. Generally, models with AUC values exceeding 0.7 are considered acceptable, while those between 0.87 and 0.9 demonstrate strong discriminative power, and values above 0.9 indicate excellent performance (Vafakhah et al., 2020). The Figure 8 illustrates the performance of the AHP model applied to flood-prone area mapping based on the AUROC.

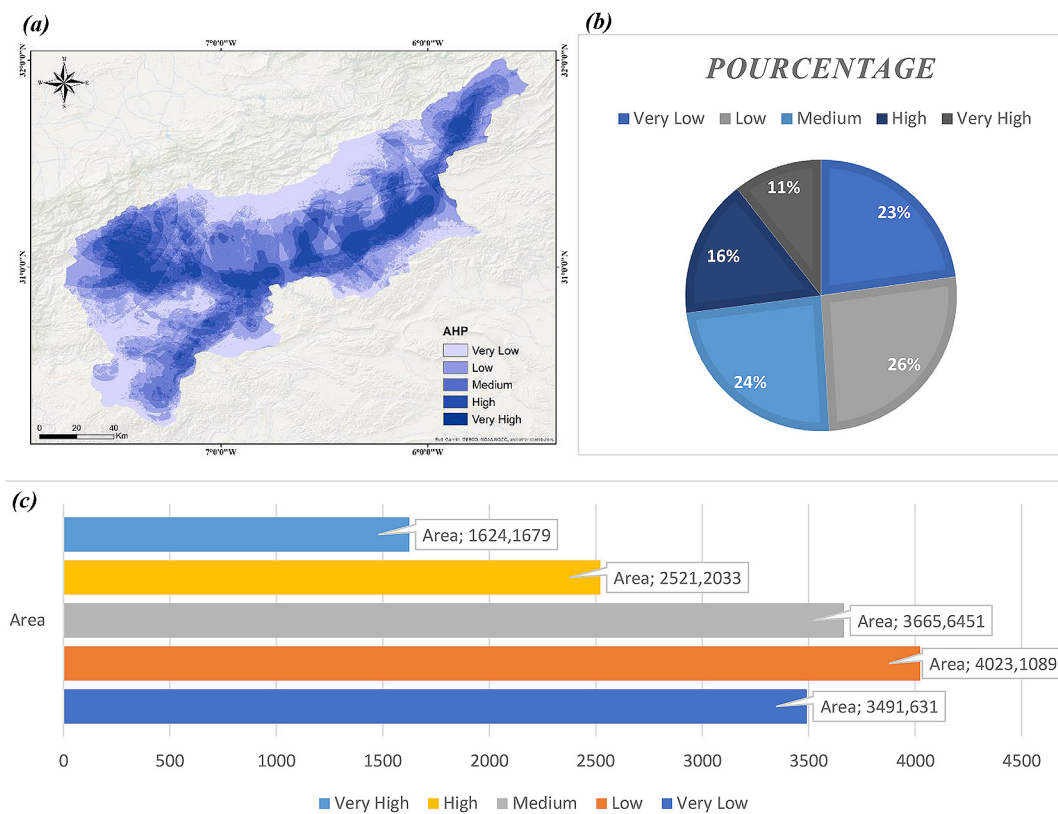


Figure 7. Flood susceptibility zonation maps based on AHP: (a) flood risk percentage, and (b, c) spatial distribution of flood susceptibility in the basin

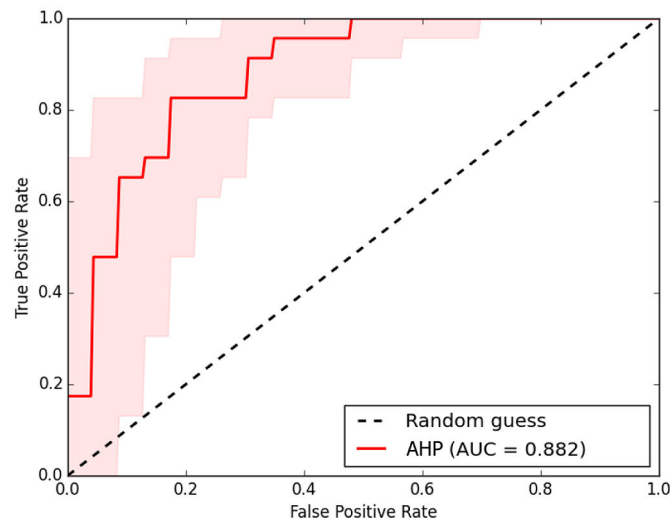


Figure 8. ROC curve evaluation susceptibility zonation map

The ROC curve, shown in red, represents the true positive rate plotted against the False Positive Rate, demonstrating the model's ability to accurately identify flood-prone areas against its tendency to classify non-flood-prone areas as flood-prone.

The AUC value of 0.882 reflects strong discriminatory power, hence indicating that the AHP model has a good distinction between flood-prone and non-flood-prone areas. This shows that the factors considered in the AHP model, such as elevation, slope, land use, and distance to rivers, were appropriately weighted to provide reliable flood susceptibility mapping. The shaded area probably represents the confidence interval, showing the range of possible model performance. Overall, this ROC curve presents the AHP model as an effective tool for the assessment and management of flood prone area mapping in the Upper Draa watershed

For the validation of flood prone mapping based on the application of AHP-MCDM in the Upper Draa watershed, historical flood inventories were employed. These inventories, detailing flood-prone areas, were supplied by the hydraulic watershed agency of Draa Oued Noun (DONHBA). Additionally, to this data, a field mission was conducted to assess flood risks within the study area. The objective of this field mission was to observe and document the areas affected by flooding, as well as to analyze the factors contributing to their vulnerability. The severe and unprecedented flooding event that occurred on the night of September 8, 2024, in the Upper Draa watershed, specifically within

the Tata, Akka, and Tamanart regions, resulted in significant socio-economic and infrastructural impacts (Figure 9). The extreme rise in water levels in the local wadis surpassed historical records, leading to the inundation and isolation of numerous villages. This flood event also caused substantial damage to essential infrastructure, further exacerbating the challenges faced by the affected communities.

DISCUSSIONS

This study emphasizes mapping flood-prone zones in the Upper Drâa watershed through an AHP-MCDM approach combined with a GIS. Seven critical factors influencing flood occurrence, including flow accumulation, elevation, slope, land use, proximity to river systems, lithology, and rainfall, were incorporated into the models. The findings underscore the necessity of prioritizing regions with high susceptibility for targeted interventions aimed at the management and restoration of wadi systems, thereby mitigating the adverse impacts of flood events. The outcomes of this study offer valuable insights that can significantly inform decision-making processes, particularly through the application of flood susceptibility zonation (FSZ) map derived from AHP. Specifically, these maps will provide critical information on the percentage of flood risk and the spatial distribution of flood risk across the basin, thereby enhancing the precision and efficacy of flood risk management strategies (refer to Figure 7).



Figure 9. Observations of flood event impact on several regains within study area [Medias-Weather]

Several studies are unanimous regarding that the arid and semi-arid zones flood risk management are more serious on account of peculiar climatic and hydrological conditions (Khaddari et al., 2023; Swain et al., 2020). Even though rainfall events are not frequent, resultant floods in such areas are often severe and lead to human losses. Therefore, there was a need for adaptive flood-risk management strategies that were able to incorporate inherent uncertainties in basin development and variability in climate. The AHP-MCDM approach used in this study yields an impressive AUC value of 0.882, demonstrating the method's effectiveness in flood susceptibility mapping. This performance is in line with findings from similar studies in Morocco and internationally, highlighting the robustness of the approach. For instance, Khaddari et al. (2023) applied the AHP-MCDM method in the Assaka watershed, Morocco, achieving accurate flood-prone area identification through a combination of multi-criteria factors such as topography, hydrology, and land use. Similarly, in India, the AHP-MCDM approach, in conjunction with GIS and remote sensing techniques, has been extensively validated. A study in Bihar, India, employed AHP to assess flood susceptibility, considering several geo-environmental factors, e.g., hydrological,

morphometrical, and anthropogenical factors, demonstrating the versatility and reliability of the method in diverse environmental conditions. In another study, Negese et al. (2022) demonstrated the effectiveness of AHP-MCDM in identifying flood-prone areas in Dega Damot, Ethiopia, with 86.83% of the region highly susceptible to flooding. This, along with similar studies, underscores the method's reliability for producing accurate flood susceptibility maps in diverse global contexts. Moreover, the current study findings can contribute to refining the hierarchy of regions with flood occurrence by identifying zones requiring urgent hydraulic studies, immediate rehabilitation efforts, such as reprofiling riverbeds and upgrading drainage systems, and the development of hydraulic infrastructure, including dykes, dams, bridges, and protective walls. Additionally, the current study highlights the importance of expansion suitability planning in facilitating informed forecasting for urban as well as rural living spaces, agricultural zones, traffic systems, and manufacturing clusters, while taking into account the occurrence of natural disasters. Additionally, supplying the primary watershed's flash flood channels, with hydrometeorological monitoring stations is proposed to enable consistent tracking of water flow and levels, complemented by the

creation of a publicly accessible web mapping platform for real-time flood event updates. While the efficacy of MCDM has been well established, the integration of more advanced techniques in future studies, mainly those leveraging AI is projected to significantly enhance the accuracy as well as the effectiveness of flood prone mapping studies. For instance, ML models can refine predictive capabilities by integrating and modeling relationships of diverse factors influencing flood dynamics. Another strategy to compliment this perspective is by a synergistic integration of RS data and real time management systems, fostering the development of a dynamic as well as a preferred high-resolution data set. Such an approach would enhance modeling approach precision, enabling also the formulation of data-driven flood prone mapping strategies in similar regions worldwide. This reflects a convergence of cutting-edge technological frameworks with interdisciplinary methodologies in bridging data science with environmental monitoring principles.

CONCLUSIONS

This research successfully applied the AHP-MCDM approach integrated within a GIS framework to map flood-susceptible areas in the Upper Drâa watershed. The study made a significant contribution in obtaining a reliable flood-prone zonation map, based on the integration of seven key factors, namely slope, flow accumulation, elevation, land use, proximity to river systems, lithology, and rainfall. These factors were weighted as well as analysed via AHP approach, yielding a FSM with high spatial accuracy, as confirmed by the strong performance evaluation. The AUC value indicates the model's robust discriminatory power, effectively identifying flood-prone zones in the studied UDB and enhancing decision-making for flood monitoring strategies. The main findings are as follows:

The FSM clearly identifies areas most prone to flooding, enabling targeted interventions in these high-susceptibility regions. These areas, which are especially vulnerable to flood events (11% of the total basin surface), should focus on the restoration of wadi systems, the construction of hydraulic infrastructure such as dams, dykes, and bridges, and urbanization planning aimed at enhancing flood resilience.

The quantitative evaluation of the integration of geospatial data and AHP-MCDM model

demonstrates its effectiveness in flood susceptibility mapping, with an AUC value of 0.8820. This high value indicates the model's strong discriminatory power in accurately identifying flood-prone zones, underpinning its reliability for decision-making processes in flood prone management realm. The performance assessment further supports the application of AHP in similar flood mapping studies.

The findings of this study are crucial for refining flood monitoring and managing practices in the UDB region. By providing an accurate zoning map, our research supports decision-makers in effectively and sustainably allocating resources for flood risk reduction. The study highlights the value of using GIS-based mapping approaches for better/sustainable flood forecasting, and mitigation planning.

This study establishes the foundation for subsequent research endeavors that seek to integrate cutting-edge technology like sophisticated artificial intelligence and real-time hydrometeorological monitoring systems. These technologies have the potential to greatly improve FSM accuracy, aid in the creation of early warning systems, and eventually increase community resilience while lowering the risk of disasters. To sum-up, this study's findings enhance flood control in the UDB and offer a paradigm that can be used in other analogous areas. Flood risk management will be greatly enhanced by the suggested incorporation of cutting-edge modeling algorithms and the conception of web-based systems for a real-time flood monitoring. This would increase community resilience and sustainable development.

REFERENCES

1. Aghenda, M., Labbaci, A., Hssaisoune, M., & Bouchaou, L. (2024). *Flood susceptibility mapping using neural network based models in Morocco: Case of Souss Watershed*. European Geosciences Union General Assembly, Vienna, Austria
2. Akay, H., & Baduna Koçyiğit, M. (2024). Investigation of flood hazard susceptibility using various distance measures in technique for order preference by similarity to ideal solution. *Applied Sciences*, 14(16), 7023.
3. Apollonio, C., Balacco, G., Novelli, A., Tarantino, E., & Piccinni, A. F. (2016). Land use change impact on flooding areas: The case study of Cervaro Basin (Italy). *Sustainability*, 8(10), 996.

4. Barkey, R., Malamassam, D., Mukhlisa, A., & Nursaputra, M. (2020). Land use planning for floods mitigation in Kelara Watershed, South Sulawesi Province, Indonesia. *IOP Conference Series: Earth and Environmental Science*,
5. Cao, Y., Jia, H., Xiong, J., Cheng, W., Li, K., Pang, Q., & Yong, Z. (2020). Flash flood susceptibility assessment based on geodetector, certainty factor, and logistic regression analyses in Fujian Province, China. *ISPRS International Journal of Geo-Information*, 9(12), 748.
6. Çavur, M., Duzgun, H., Kemeç, S., & Demirkan, D. (2019). Land use and land cover classification of Sentinel 2-A: St Petersburg case study. *The International Archives of Photogrammetry, Remote Sensing and Spatial Information Sciences*, 42, 13-16.
7. Choubert, G. (1952). Histoire géologique du domaine de l'Anti-Atlas. *Notes et Mém. Serv. Géol. Maroc*, 100, 77-172.
8. Costache, R., & Bui, D. T. (2020). Identification of areas prone to flash-flood phenomena using multiple-criteria decision-making, bivariate statistics, machine learning and their ensembles. *Science of The Total Environment*, 712, 136492.
9. Das, S. (2018). Geographic information system and AHP-based flood hazard zonation of Vaitarna basin, Maharashtra, India. *Arabian Journal of Geosciences*, 11(19), 576.
10. Das, S., & Gupta, A. (2021). Multi-criteria decision based geospatial mapping of flood susceptibility and temporal hydro-geomorphic changes in the Subarnarekha basin, India. *Geoscience Frontiers*, 12(5), 101206.
11. Dash, P., & Sar, J. (2020). Identification and validation of potential flood hazard area using GIS-based multi-criteria analysis and satellite data-derived water index. *Journal of Flood Risk Management*, 13(3), e12620.
12. Devito, K., Creed, I., Gan, T., Mendoza, C., Petrone, R., Silins, U., & Smerdon, B. (2005). A framework for broad-scale classification of hydrologic response units on the Boreal Plain: Is topography the last thing to consider? *Hydrological Processes: An International Journal*, 19(8), 1705–1714.
13. Dey, H., Shao, W., Haque, M. M., & VanDyke, M. (2024). Enhancing Flood Risk Analysis in Harris County: Integrating Flood Susceptibility and Social Vulnerability Mapping. *Journal of Geovisualization and Spatial Analysis*, 8(1), 19.
14. Echogdali, F., Boutaleb, S., Jauregui, J., & Elmouden, A. (2018). Cartography of flooding hazard in semi-arid climate: the case of Tata Valley (South-East of Morocco). *J Geogr Nat Disast.*, 8(214), 2167–0587.1000214.
15. El Jazouli, A., Barakat, A., & Khellouk, R. (2019). GIS-multicriteria evaluation using AHP for landslide susceptibility mapping in Oum Er Rbia high basin (Morocco). *Geoenvironmental Disasters*, 6(1), 1–12.
16. El Morjani, Z., Seif Ennasr, M., Elmouden, A., Idbraim, S., Bouaakaz, B., & Saad, A. (2016). Flood hazard mapping and modeling using GIS applied to the Souss river watershed. *The Souss-Massa River Basin, Morocco*, 57–93.
17. Horton, R. E. (1932). Drainage-basin characteristics. *Transactions, American geophysical union*, 13(1), 350–361.
18. Ikirri, M., Faik, F., Echogdali, F. Z., Antunes, I. M. H. R., Abioui, M., Abdelrahman, K., Fnais, M. S., Wanaim, A., Id-Belqas, M., & Boutaleb, S. (2022). Flood hazard index application in arid catchments: Case of the taguenit wadi watershed, Lakhssas, Morocco. *Land*, 11(8), 1178.
19. Ivan Ulloa, N., Chiang, S.-H., & Yun, S.-H. (2020). Flood proxy mapping with normalized difference sigma-naught index and Shannon's entropy. *Remote Sensing*, 12(9), 1384.
20. Khaddari, A., Bouziani, M., Moussa, K., Sammar, C., Chakiri, S., Hadi, H., Jari, A., & Titafi, A. (2022). Evaluation of Precipitation Spatial Interpolation Techniques using GIS for Better Prevention of Extreme Events: Case of the Assaka Watershed (Southern Morocco). *Eco. Env. & Cons*, 28, 1–10.
21. Khaddari, A., Jari, A., Chakiri, S., El Hadi, H., Labriki, A., Hajaj, S., El Harti, A., Goumghar, L., & Abioui, M. (2023). A comparative analysis of analytical hierarchy process and fuzzy logic modeling in flood susceptibility mapping in the Assaka Watershed, Morocco. *Journal of Ecological Engineering*, 24(8), 62–83.
22. Khettouch, A., Hssaisoune, M., Hermans, T., Aouijil, A., & Bouchaou, L. (2023). Ground validation of satellite-based precipitation estimates over poorly gauged catchment: the case of the Drâa basin in Central-East Morocco. *Mediterranean Geoscience Reviews*, 5(3), 159–175.
23. Khoirunisa, N., Ku, C.-Y., & Liu, C.-Y. (2021). A GIS-based artificial neural network model for flood susceptibility assessment. *International Journal of Environmental Research and Public Health*, 18(3), 1072.
24. Khosravi, V., Shirazi, A., Shirazy, A., Hezarkhani, A., & Pour, A. B. (2021). Hybrid fuzzy-analytic hierarchy process (AHP) model for porphyry copper prospecting in simorgh area, eastern lut block of Iran. *Mining*, 2(1), 1–12.
25. Leta, B. M., & Adugna, D. (2023). Identification and mapping of flood-prone areas using GIS-based multi-criteria decision-making and analytical hierarchy process: the case of Adama City's watershed,

- Ethiopia. *Applied Geomatics*, 15(4), 933–955.
26. Mashaly, J., & Ghoneim, E. (2018). Flash flood hazard using optical, radar, and stereo-pair derived dem: Eastern desert, Egypt. *Remote Sensing*, 10(8), 1204.
 27. Melton, M. A. (1957). *An analysis of the relations among elements of climate, surface properties, and geomorphology* (Vol. 11). Department of Geology, Columbia University New York.
 28. Mitra, R., Saha, P., & Das, J. (2022). Assessment of the performance of GIS-based analytical hierarchical process (AHP) approach for flood modelling in Uttar Dinajpur district of West Bengal, India. *Geomatics, Natural Hazards and Risk*, 13(1), 2183–2226.
 29. Muthu, K., & Ramamoorthy, S. (2024). Evaluation of urban flood susceptibility through integrated Bivariate statistics and geospatial technology. *Environmental Monitoring and Assessment*, 196(6), 526.
 30. Negese, A., Worku, D., Shitaye, A., & Getnet, H. (2022). Potential flood-prone area identification and mapping using GIS-based multi-criteria decision-making and analytical hierarchy process in Dega Damot district, northwestern Ethiopia. *Applied Water Science*, 12(12), 255.
 31. Nithya, C. N., Srinivas, Y., Magesh, N., & Kaliraj, S. (2019). Assessment of groundwater potential zones in Chittar basin, Southern India using GIS based AHP technique. *Remote Sensing Applications: Society and Environment*, 15, 100248. <https://doi.org/10.1016/j.rsase.2019.100248>
 32. Panchal, S., & Shrivastava, A. K. (2022). Landslide hazard assessment using analytic hierarchy process (AHP): A case study of National Highway 5 in India. *Ain Shams Engineering Journal*, 13(3), 101626.
 33. Pusdekar, P. N., & Dudul, S. V. (2024). Flood Susceptibility Mapping and Accuracy Assessment of a River Floodplain Using Bivariate Statistical Methods and AHP Approach. 2024 International Conference on Emerging Smart Computing and Informatics (ESCI),
 34. Radwan, F., Alazba, A., & Mossad, A. (2019). Flood risk assessment and mapping using AHP in arid and semiarid regions. *Acta Geophysica*, 67, 215–229.
 35. Roy, S., Bose, A., & Chowdhury, I. R. (2021). Flood risk assessment using geospatial data and multi-criteria decision approach: a study from historically active flood-prone region of Himalayan foothill, India. *Arabian Journal of Geosciences*, 14(11), 999.
 36. Saaty, T. L. (1980). A scaling method for priorities in hierarchical structures. *Journal of mathematical psychology*, 15(3), 234–281.
 37. Saha, S., Sarkar, D., & Mondal, P. (2022). Efficiency exploration of frequency ratio, entropy and weights of evidence-information value models in flood vulnerability assessment: a study of raiganj subdivision, Eastern India. *Stochastic Environmental Research and Risk Assessment*, 36(6), 1721–1742.
 38. Samanta, R. K., Bhunia, G. S., Shit, P. K., & Pourghasemi, H. R. (2018). Flood susceptibility mapping using geospatial frequency ratio technique: a case study of Subarnarekha River Basin, India. *Modeling Earth Systems and Environment*, 4, 395–408.
 39. Samanta, S., Pal, D. K., & Palsamanta, B. (2018). Flood susceptibility analysis through remote sensing, GIS and frequency ratio model. *Applied Water Science*, 8(2), 66.
 40. Saremi, M., Maghsoudi, A., Hoseinzade, Z., & Mokhtari, A. R. (2024). Data-driven AHP: a novel method for porphyry copper prospectivity mapping in the Varzaghan District, NW Iran. *Earth Science Informatics*, 1–16.
 41. Sarker, S. C., Monir, M. M., & Islam, M. N. (2024). Analyzing Spatiotemporal changes in flood risk zones to mitigate flood hazards in a floodplain area using a GIS-based AHP technique. In: *Flood Risk Management: Assessment and Strategy* (pp. 23–47). Springer.
 42. Shafapour Tehrany, M., Kumar, L., Neamah Jebur, M., & Shabani, F. (2019). Evaluating the application of the statistical index method in flood susceptibility mapping and its comparison with frequency ratio and logistic regression methods. *Geomatics, Natural Hazards and Risk*, 10(1), 79–101.
 43. Shikhteymour, S. R., Borji, M., Bagheri-Gavkosh, M., Azimi, E., & Collins, T. W. (2023). A novel approach for assessing flood risk with machine learning and multi-criteria decision-making methods. *Applied Geography*, 158, 103035.
 44. Song, J. Y., & Chung, E.-S. (2016). Robustness, uncertainty and sensitivity analyses of the TOPSIS method for quantitative climate change vulnerability: a case study of flood damage. *Water Resources Management*, 30, 4751–4771.
 45. Swain, K. C., Singha, C., & Nayak, L. (2020). Flood susceptibility mapping through the GIS-AHP technique using the cloud. *ISPRS International Journal of Geo-Information*, 9(12), 720.
 46. Tanguy, M. (2012). Cartographie du risque d'inondation en milieu urbain adaptée à la gestion de crise: Analyse préliminaire.
 47. Teh Noranis, M. A., Maslina, Z., & Noraini, C. P. (2019). Fuzzy AHP in a knowledge-based framework for early flood warning. *Applied Mechanics and Materials*, 892, 143–149.
 48. Tehrany, M. S., Pradhan, B., & Jebur, M. N. (2015). Flood susceptibility analysis and its verification using a novel ensemble support vector machine and frequency ratio method. *Stochastic Environmental Research and Risk Assessment*, 29, 1149–1165.

49. Tehrany, M. S., Pradhan, B., Mansor, S., & Ahmad, N. (2015). Flood susceptibility assessment using GIS-based support vector machine model with different kernel types. *CATENA*, 125, 91–101.
50. Vafakhah, M., Mohammad Hasani Loor, S., Pourghasemi, H., & Katebikord, A. (2020). Comparing performance of random forest and adaptive neuro-fuzzy inference system data mining models for flood susceptibility mapping. *Arabian Journal of Geosciences*, 13, 1–16.
51. Vignesh, K., Anandakumar, I., Ranjan, R., & Borah, D. (2021). Flood vulnerability assessment using an integrated approach of multi-criteria decision-making model and geospatial techniques. *Modeling Earth Systems and Environment*, 7(2), 767–781.
52. Wang, Y., Hong, H., Chen, W., Li, S., Pamučar, D., Gigović, L., Drobnjak, S., Tien Bui, D., & Duan, H. (2018). A hybrid GIS multi-criteria decision-making method for flood susceptibility mapping at Shangyou, China. *Remote Sensing*, 11(1), 62.
53. Zou, Q., Zhou, J., Zhou, C., Song, L., & Guo, J. (2013). Comprehensive flood risk assessment based on set pair analysis-variable fuzzy sets model and fuzzy AHP. *Stochastic Environmental Research and Risk Assessment*, 27, 525–546.